

NonGEMM Bench: Understanding the Performance Horizon of the Latest ML Workloads with NonGEMM Workloads

RACHID KARAMI, UC Irvine, USA
HEMANTH KOTA, UC Irvine, USA
SHENG-CHUN KAO, Google, USA
HYOUKJUN KWON, UC Irvine, USA

Abstract: Machine Learning (ML) operators are the building blocks to design ML models with various target applications. General Matrix Multiplication (GEMM) operators are the backbone of ML models. They are notorious for being computationally expensive requiring billions of multiply-and-accumulate. Therefore, significant effort has been put to study and optimize the GEMM operators in order to speed up the execution of ML models. GPUs and accelerators are widely deployed to accelerate ML workloads by optimizing the execution of GEMM operators. Nonetheless, the performance of NonGEMM operators have not been studied as thoroughly as GEMMs. Therefore, this paper describes NONGEMM BENCH, a benchmark to study NonGEMM operators. We first construct NONGEMM BENCH using popular ML workloads from different domains, then perform case studies on various grade GPU platforms to analyze the behavior of NonGEMM operators in GPU accelerated systems. Finally, we present some key takeaways to bridge the gap between GEMM and NonGEMM operators and to offer the community with potential new optimization directions.

ACM Reference Format:

Rachid Karami, Hemanth Kota, Sheng-Chun Kao, and Hyoukjun Kwon. 2024. NonGEMM Bench: Understanding the Performance Horizon of the Latest ML Workloads with NonGEMM Workloads. 1, 1 (April 2024), 21 pages. <https://doi.org/10.1145/nnnnnnn.nnnnnnn>

1 INTRODUCTION

The success of machine learning (ML) in various problem domains, such as computer vision [13, 14, 18, 21, 27] and natural language processing [5, 17, 28], made ML workloads pervasive in various computing platforms from edge to cloud devices. ML models typically involve billions of multiply-and-accumulate (MAC) operations (e.g., 497 billions of MAC operations for ResNet 50 [14]). Among many operators used in ML models, GENERAL MATRIX MULTIPLICATION (GEMM)-based operators, such as CONV2D, FC (fully-connected layer), Linear, and BMM (batched matrix multiplication) dominate in terms of the computational cost, as presented in Figure 1. Therefore, GPUs and accelerators have focused on the optimization of the GEMM-based operators and greatly enhanced the computational performance (e.g., latency and throughput) and energy efficiency of end-to-end ML model inference.

However, because the GEMM operators are being accelerated, the non-GEMM operators, such as memory operations (e.g., reshape, view, and transpose), normalization, and logit computation functions (e.g., Softmax), now account for a considerable amount of the end-to-end latency, compared to that of GEMM operators. Figure 1 shows the profiled latency breakdown into GEMM and non-GEMM operators running inferences on state-of-the-art large language (GPT2-XL [5]) and

Authors' addresses: Rachid Karami, UC Irvine, Irvine, CA, USA; Hemanth Kota, UC Irvine, Irvine, CA, USA; Sheng-Chun Kao, Google, MTW, CA, USA; Hyoukjun Kwon, UC Irvine, Irvine, CA, USA.

Permission to make digital or hard copies of all or part of this work for personal or classroom use is granted without fee provided that copies are not made or distributed for profit or commercial advantage and that copies bear this notice and the full citation on the first page. Copyrights for components of this work owned by others than the author(s) must be honored. Abstracting with credit is permitted. To copy otherwise, or republish, to post on servers or to redistribute to lists, requires prior specific permission and/or a fee. Request permissions from permissions@acm.org.

© 2024 Copyright held by the owner/author(s). Publication rights licensed to ACM.

ACM XXXX-XXXX/2024/4-ART

<https://doi.org/10.1145/nnnnnnn.nnnnnnn>

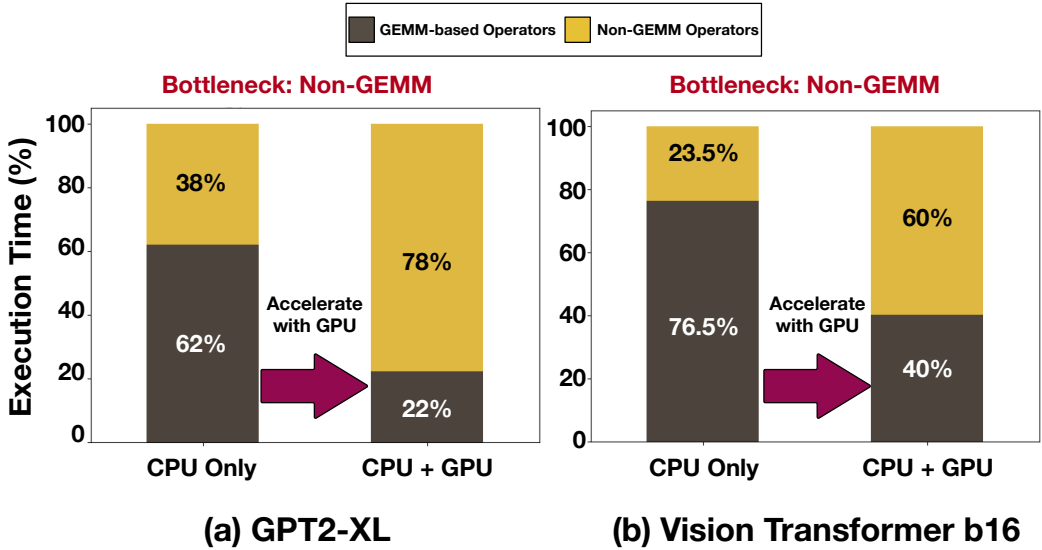


Fig. 1. The latency breakdown into GEMM and non-GEMM operators on AMD EPYC 7763 + NVIDIA A100 GPU. We measure the latency on two popular models from HuggingFace (a) GPT2-XL (batch 1) [5] and (b) Vision Transformer (batch 1) [18].

image classification (Vision Transformer [18]) models. The motivational data imply a major shift of the landscape of Amdahl’s law for ML acceleration, indicating that we now need to consider non-GEMM operators in the ML system optimization. However, no study thoroughly explored the non-GEMM operator performance in latest models, although it is important to quantitatively understand the current status.

Therefore, we propose **NONGEMM BENCH**, which focuses on non-GEMM operator analysis in popular ML models today. Unlike previous benchmarks, **NONGEMM BENCH** thoroughly analyzes NonGEMM operator performance, which provides important insights on the ML system optimization with powerful accelerators. **NONGEMM BENCH** consists of 18 distinct models collected from Hugging Face and Torchvision on various computer vision and natural language processing tasks, and the models were selected based on their popularity, which makes **NONGEMM BENCH** aligned with the realistic use cases.

To deliver more insights in NonGEMM operators, **NONGEMM BENCH** provides a microbenchmark suite of NonGEMM operators. **NONGEMM BENCH** supports arbitrary NonGEMM operators in any models supported by PyTorch FX [24], which is compatible with a majority of the ML models. The flow allows users to analyze any NonGEMM operators without manually writing custom functions, unlike previous benchmark [19]. In addition, **NONGEMM BENCH** provides input argument specification extracted from real data. This helps analyze NonGEMM operators in realistic settings, which is crucial for some operators whose behavior is heavily dependent on input arguments

Using this benchmark, we perform case studies on 18 popular Hugging Face and Torchvision models on image classification, object detection, segmentation, and generative language models (e.g., Llama 2 [28] and GPT-2 [22]). We study the performance on seven different hardware configuration ranging from mobile, desktop, to data center, which includes four CPU and three GPU models. In our case studies, we evaluate the effect of GPU acceleration on the latency distribution across

operators for the selected models highlighting the contribution of NonGEMM operators to the end to end latency of the accelerated model.

We will open-source NONGEMM BENCH at the time of publication to facilitate the ML system research aligned with the current performance horizon. Including that, we make the following contributions:

- We shed a light on the changed landscape of Amdhal’s law in ML system design.
- We propose NONGEMM BENCH, which provides detailed analysis on NonGEMM operators in the 16 latest popular models collected from Hugging Face and Torchvision.
- To facilitate NonGEMM operator-aware optimizations, we organize a microbenchmark of NonGEMM operators collected in the popular models and provide realistic input arguments collected from realistic input data.
- Using NONGEMM BENCH, we perform case studies on seven different hardware configurations ranging from mobile, desktop, to data center, and show the change in the impact of NonGEMM operators on the execution time of the models.

2 BACKGROUND

2.1 ML Operators

ML operators constitute the building blocks for creating machine learning models. Operators consist of a computation or operation that generates an output tensor from an input tensor. Examples include compute-intensive operators such as convolution (CONV2D) and matrix multiplication (linear, BMM, etc.), and other less expensive (computationally) operators like activation (RELU), and normalization functions (LayerNorm) for example. The combination of ML operators with weights (if applicable) creates layers, which are often cascaded many times to make the machine learning model deep. The various permutations of operators and layers define the architecture of the deep neural network (DNN).

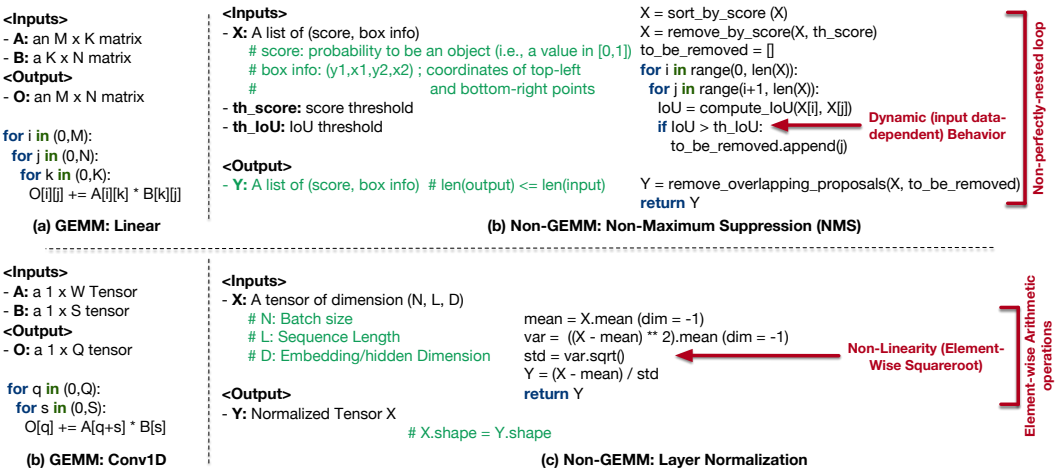


Fig. 2. A description of Linear (a) and Conv1D (c) operators as GEMM operators example, and that of non-maximum suppression [13] (b) and Layer Normalization [6] (d) as a non-GEMM operator example.

2.1.1 GEMM-based operations. GEMM operators are computationally heavy operators based on General Matrix Multiplication (GEMM) operations which compute MAC operations inside

tightly nested loops typically causing them to dominate the ML workload. Matrix Multiplication, Convolution (CONV1D and CONV2D) and Linear (fully connected) layers are examples of the mostly used GEMM operators in DNN. Figure 2 (a) and Figure 2 (c) illustrate the algorithms of Linear and CONV1D operators respectively. Both operators loop over the input tensor dimensions and populate the output tensor by computing a MAC inside the inner most loop. Despite having different semantics, GEMM operators compute MACs in tightly nested loops and can be expressed as a series of matrix multiplications or dot products. For example, 2-dimensional convolution can be mapped to a matrix multiplication as shown in [9], and linear layers compute a vector-matrix multiplication between an input feature tensors and the layers' weights.

2.1.2 Non-GEMM Operators. Non-GEMM operators are building blocks found in ML models that are different than GEMMs. They span different functionalities and unlike GEMMs, they are not centered around a common architecture (e.g. tight loop nest with MAC). They encompass memory operations, as well as non-linear functions (e.g. element-wise Squareroot in Layer Normalization shown in Figure 2 (d)). Some operators also introduce non deterministic behaviors through conditional statements, like non-maximum suppression which algorithm is shown in Figure 2 (b). We label non-GEMM operators based on their functionality and summarize them according to the groups in Table 2.

- **Normalization** functions were introduced to regularize the input across a certain dimension. Batch Norm [16] and Layer Norm [6] are traditional normalization functions heavily used in DL models from computer vision and NLP applications [5], [13]. Both of these functions normalize the intermediate feature tensors by computing the mean and standard deviation statistics over a specific tensor dimension. For a tensor with dimensions (Batch, Channel, Height, Width), Batch Norm normalizes over the batch dimension B while Layer Norm performs the normalization across the last dimension of the tensor (Figure 2 (d)). RMS Norm [31] is another function that has been recently used in the large language model Llama [28] that regularizes the feature tensors based on the value of the root mean square.
- **Activation** Functions introduce non linearity into the model. Activation functions span from the straightforward ReLU which filters out negative tensor values, to the more sophisticated GELU [15] suggesting a probabilistic gaussian approach to dropping data points.
- **Memory Operations** consist of operations related to the allocation and the "view" of a tensor inside the memory. A tensor "view" operation does not modify the original input tensor in memory nor creates a new copy. It provides the user with a new "view" of the tensor with new dimensions by modifying the tensor shape and the strides to access the elements. Operators dealing with indexing, reshaping and concatenating tensors fall into this category as well. An example of memory operations would be the Pytorch reshape function used in the implementation of the attention block in Hugging Face transformers library to ensure the correct dimensions of the Key matrix before multiplying it with the Query matrix.
- **Element-Wise Arithmetic** operators cover all element wise arithmetic tensor operations. An example would be applying element wise division to scale the elements of tensors in the attention block as shown in Figure 3.
- **RoI Selection** functions are used in FasterRCNN [25] and MaskRCNN [13] detection models. They filter down bounding boxes proposed by the region proposal network (Figure 3 (b)) and align the filtered boxes to the objects detected in the image. Non-Maximum Suppression (NMS) is an RoI selection operator used in RCNN models described in Figure 2. Given a list of scores and bounding box information, it drops bounding boxes based on a threshold score then filters out overlapping boxes based on the Intersection over Union (IoU) metric.

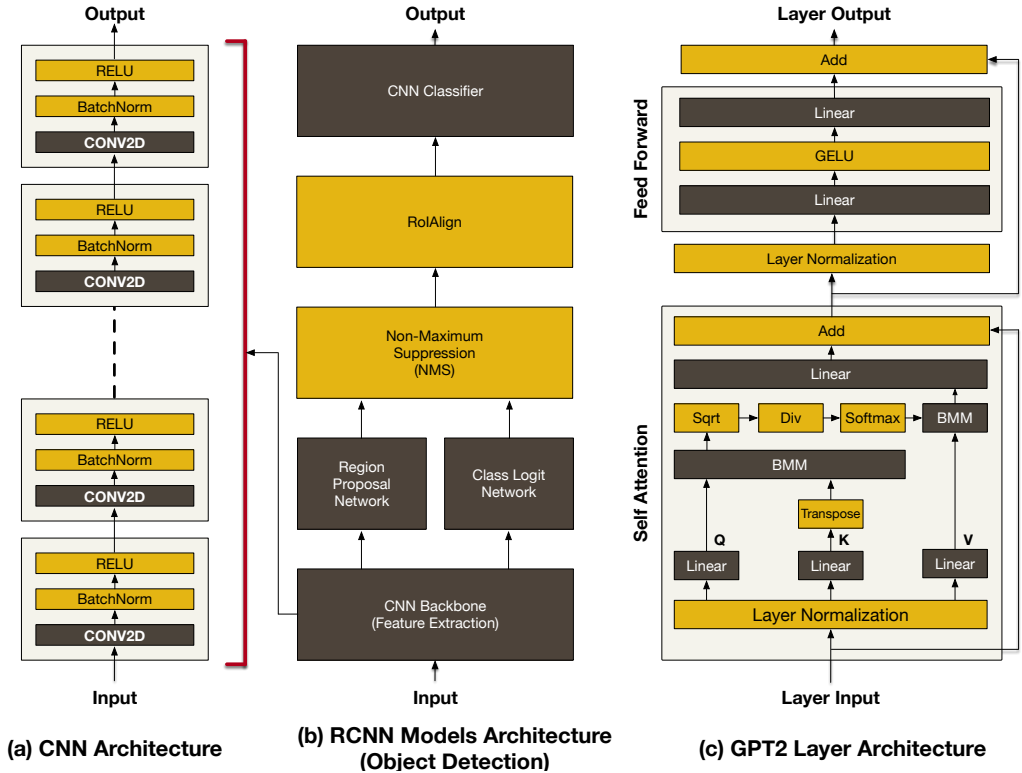


Fig. 3. The architecture of three popular families of ML models.

2.2 ML Models and Popular Tasks

The diversity in operators equipped ML algorithm designers with the building blocks required to architect models excelling in a wide range of tasks. Computer Vision (CV) and NLP are domains where deep learning has succeeded and shown great potential. Therefore, developers have designed models with specific architectures leveraging distinct operators for each task in CV and NLP. Figure 3 shows the difference in architecture and operators used for models from different tasks. Classical models in image classification consist of deep convolution networks made by deeply cascading blocks of CONV2D, normalization and activation operators [27]. Object Detection models also rely on deep convolution network as a backbone and they pair it with different heads and operators to as shown in Figure 3. On the other hand, NLP and language models rely on a completely different architecture. They use transformer models and attention mechanism introduced in [29]. Figure 3 describe a decoder only transformer architecture which is used in popular language models like GPT.

In NONGEMM BENCH, we collect models from the computer vision and NLP domains to break-down their performance and understand the contributions of each operator, especially the non-GEMM ones.

3 NONGEMM BENCH

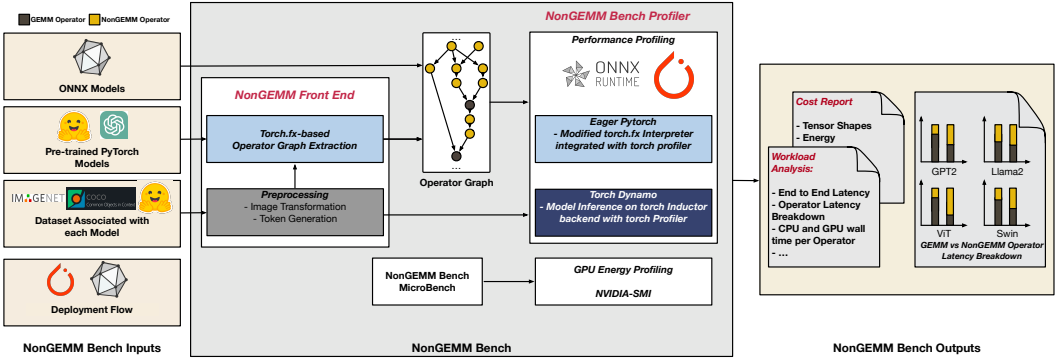


Fig. 4. Overview of the different stages of NONGEMM BENCH

To better understand the performance of ML models across application domains, we collect popular CV and NLP models and we evaluate their performance on different target platforms. To gain more insight on their operator structure and how the operator type is affecting performance, NONGEMM BENCH allows the user to profile the models at the operator level. Unlike LongTail bench that focuses on micro-benchmarking operators without an ATEN or cuda kernel [19], NONGEMM BENCH allows the user to breakdown the model’s performance at the computational graph level in end to end inference scenarios. Moreover, NONGEMM BENCH can also provide a finer breakdown of the lower level kernels implementing the graph operators hence, exhibiting macro and micro benchmarking capabilities. In the rest of this section, we present NONGEMM BENCH and describe its model selection process and different benchmarking flows.

3.1 NONGEMM BENCH Model Description

To make sure NONGEMM BENCH captures the latest ML workloads, we select 18 highly-downloaded models from HuggingFace [1] for the representativeness of NONGEMM BENCH. NONGEMM BENCH covers four major task domains in ML, which include image classification, object detection, image segmentation, and natural language processing.

As listed in Table 1, NONGEMM BENCH includes 18 models based on state-of-the-art CNN and Transformer architecture. The number of parameters of the models ranges from 0.85M to 7B, which shows the diverse model coverage of NONGEMM BENCH. NONGEMM BENCH also includes variants of the same models (e.g., ViTBase16, ViT large16, and ViT huge variants of the Vision Transformer [18]), which target diverse use cases in different platforms (e.g., smartphone, workstation, and data center).

3.1.1 Computer Vision. Deep Learning is widely used in the computer vision domain [18] [14] [25]. NONGEMM BENCH covers three important task domain of the computer vision as follows:

- **Image Classification (IC):** Image classification refers to a computer vision task that identifies a class label of a given image. Image classification models extract features (i.e., high-level and -dimensional information of the input image) from an input image and reports the class label utilizing the features. NONGEMM BENCH includes eight most popular IC models in HuggingFace [1], which includes ResNet50 [14], MobileNetv2 [27], three variants of Vision Transformer [18], and three variants of Swin Transformer [21].
- **Image Segmentation (IS):** Image segmentation refers to a computer vision task that identifies the area in a image for each class. Like IC models, IS models also extract features and utilize them to identify objects located in an image and spatially separate them by highlighting

pixels belong to each object. NONGEMM BENCH includes two state-of-the-art IS models: Segformer [30] and MaskFormer [8].

- **Object Detection (OD):** Object detection refers to a computer vision task that identifies the location of objects in an image and outputs the bounding box of each object. Like aforementioned models, OD models extract features. In addition to that, OD models generate region proposal, which refers to the candidate location and bounding boxes for objects in an image. Using RoI processing non-GEMM operators listed in Table 2, OD models refine the raw region proposal generated by a region proposal network. The refined RoIs are used as inputs to the classifier CNN at the end, and the classifier determines the class label of object inside each redefined RoI. NONGEMM BENCH includes three popular OD models [2]: FasterRCNN [25], MaskRCNN [13], and DETR [7].

3.1.2 Natural Language Processing. Natural Language Processing (NLP) refers to tasks involving the analysis and understanding of human (natural) language. Transformer [29] based DNNs have become the most dominant neural network models in NLP. They are the backbone of popular state of the art generative large language models like GPT [22] and Llama [28]. Figure 3 (c) shows the layer architecture of GPT’s transformer. It consists of diverse GEMM and NonGEMM operators implementing a self attention block followed by a feed forward network. NONGEMM BENCH includes five popular NLP models [3]: Bert [17], three variants of GPT2 [5], and Llama2-7b [28].

3.1.3 Datasets. To evaluate the collected models, NONGEMM BENCH utilizes real data from popular datasets in each domain. We use ImageNet 2012 [10] and MS COCO [20] for computer vision tasks. As for language models, we use wikitext dataset available on HuggingFace [4].

3.2 Benchmark Suite

NONGEMM BENCH profiling flow runs the model with inputs from real datasets and captures the latency performance at the operator level. Additional operator data (e.g. input tensor shapes) is extracted and used to drive NONGEMM BENCH microbench flow. NONGEMM BENCH microbench flow analyzes the energy cost of non-GEMM operators by using input tensors with dimensions based on real data collected during the profiling flow.

3.2.1 NONGEMM BENCH Frontend. In the first stage of NONGEMM BENCH, we start by preprocessing the inputs retrieved from the appropriate dataset. The data is fetched in its raw format as images or text. Tokenization is applied to text data and transformations are applied to images to obtain the input tensors. The graph is then generated using the torch FX (FX) [24] library from Pytorch. The FX tracer is the tool used to generate the computational graphs of NONGEMM BENCH models. It performs a symbolic execution using a proxy data structure to capture the operators and construct the graph nodes. A limitation of the FX tracer is its inability to trace through modules with dynamic control flow. The tracer fails if the model has a conditional or iterative statement which depends on the inputs or dynamically computed intermediate tensors. Hence, as shown in Figure 4, the preprocessed inputs are also fed into the graph generation tool to overcome the FX tracer’s limitation. By utilizing the inputs to evaluate dynamic control flow conditional statements, the tracer completes NONGEMM BENCH’s frontend by generating an input dependent operator graph.

3.2.2 NONGEMM BENCH Profiler. After obtaining the computational graph, the model is ready to be analyzed and profiled. We implement a custom Profiling Interpreter by integrating the Pytorch Profiler with the FX Interpreter to enable performance analysis at the graph node level as we evaluate the model. The base FX Interpreter iterates over the computational graph and runs the nodes in Pytorch eager mode sequentially to execute the model. The custom interpreter also

Table 1. NONGEMM BENCH Tasks and Models

Domain	Application	Models	Model Size (# Params.)	Dataset
Computer Vision	Image Classification	ResNet50	0.85M	ImageNet
		MobileNetv2	3.4M	ImageNet
		ViT Base 16	86M	ImageNet
		ViT large 16	307M	ImageNet
		ViT huge 14	632M	ImageNet
		Swin Transformer tiny	29M	ImageNet
		Swin Transformer small	50M	ImageNet
	Swin Transformer base	88M	ImageNet	
	Object Detection	FasterRCNN	42M	COCO
		MaskRCNN	44M	COCO
		DETR	41M	COCO
	Segmentation	Maskformer	102M	COCO
		SegFormer	3.7M	COCO
NLP	Language Models	GPT2	117M	wikitext
		GPT2 Large	762M	wikitext
		GPT2 X-Large	1.5B	wikitext
		Llama 2-7B	7B	wikitext
		Bert	110M	wikitext

executes the model by computing the graph’s nodes iteratively. During the computation of each node, it calls the Pytorch Profiler to instrument the node’s execution, recording the performance metrics of each operator at the low level kernel granularity.

3.2.3 NONGEMM BENCH Post Processing. After the completion of NONGEMM BENCH profiling stage, Post Processing cleans and aggregates the collected data into performance reports and visualization plots. This stage groups the operators into categories based on the operator functionality and reports the performance analysis. The reports show a breakdown of the latency across operators and devices (CPU/GPU) as well as additional information about the number of FLOPS and input tensor shapes.

3.2.4 NonGEMM Operator MicroBenchmark. Based on the workload analysis obtained by running NONGEMM BENCH, we notice a shift in the latency distribution between GEMM and NonGEMM operators after accelerating the inference (discussed in details in Section 4). The latency for NonGEMM operators is becoming more significant which indicates new potential bottleneck operators. To better study the potential bottlenecks, we identify the NonGemm operators with the highest contributions to the models latency, and construct a microbenchmark summarized in Table 2 with the operators that had the highest contributions to the models latency. The microbenchmark highlights the non-GEMM operators their implementation library and realistic input tensors sizes based on the datasets used in the profiling stage.

4 CASE STUDIES

In this section, we perform a thorough analysis of the performance data generated by running NONGEMM BENCH on multiple hardware platforms show in Table 3. We collect the data by running NONGEMM BENCH on three systems configuration ranging from mobile CPUs to data center grade CPUs and GPUs to capture the behavior of the operators when subjected to different acceleration

Table 2. A list of non-GEMM operators collected from eight popular model variants selected from Hugging Face listed in Table 1.

Operator Group	Operator	Model	Implementation	Example Input Tensor Shape
Activation	ReLU	DETR	Torch.nn.modules.activation	[2,64,533]
	GELU	ViT-l16	Torch.nn.modules.activation	[1, 97, 4096]
	GELU	GPT2-XL	transformers.activations.GELUActivation	[1, 8, 6400]
	SiLU	Llama-2	Torch.nn	[1, 10, 11008]
Normalization	LayerNorm	Segformer	Torch.nn.modules.normalization	[2, 16384, 32]
	BatchNorm2d	Segformer	Torch.nn.modules.batchnorm	[2, 256, 128, 128]
	LlamaRMSNorm	Llama	transformers.models.llama	[1, 10, 4096]
	FrozenBatchNorm2d	MaskRCNN	torchvision.ops.misc	[1, 1024, 50,68]
	FrozenBatchNorm2d	DETR	transformers.models.detr	[2, 850, 256]
Elem-wise Arithmetic	LayerNorm	DETR	Torch.nn.modules.normalization	[2, 850, 256]
	Add	Segformer	Torch.add	[2, 16384, 32]
	Mul	Llama-2	Torch.mul	[1, 10, 11008]
	Neg	Llama-2	Torch.neg	[1, 32, 10, 64]
	TrueDiv	Torch.true_divide	Segformer	[2, 1, 16384, 256]
Memory	TrueDiv	GPT2-XL	Torch.true_divide	[1, 25, 8, 8]
	Contiguous	Segformer	Torch.Tensor.contiguous	[2, 32, 128, 128]
	Contiguous	Llama-2	Torch.Tensor	[1, 10, 32, 128]
	Permute	ViT-b16	Torch.permute	[1, 768, 196]
	Permute	GPT2-XL	Torch.permute	[1, 8, 25, 64]
	Split	GPT2-XL	Torch.split	[1, 8, 4800]
	View	GPT2-XL	Torch.Tensor.view	[1, 8, 1600]
	Reshape	ViT-b16	Torch.reshape	[1, 768, 14, 14]
	Expand	ViT-b16	Torch.Tensor.expand	[1, 1, 768]
	Squeeze	Llama-2	Torch.squeeze	[1, 1, 10, 128]
Logit Computation	Softmax	DETR	Torch.nn.functional.softmax	[1, 25, 8, 8]
	Softmax	Segformer	Torch.nn.functional.softmax	[2, 1, 16384, 256]
RoI Selection	NMS	MaskRCNN	torchvision.ops.nms	[4663, 4]
Interpolation	Interpolate	Segformer	Torch.nn.functional	[2, 256, 128, 128]

Table 3. Hardware platform configurations used for NonGEMM BENCH case studies.

Class	CPU	GPU
Data Center	AMD EPYC 7763	NVIDIA A100
Workstation	Intel i9-13900K	NVIDIA RTX 4090
Mobile	Intel i7-13700HU	NVIDIA RTX 4060m
Mobile	Apple M2 Max	Apple M2 Max GPU ¹

capabilities. We notice that for most of the models, the time spent to compute non-GEMM operators increases noticeably with respect to the total execution time when running the model on the GPU.

4.1 Image Classification

As can be seen in Figure 5, there is a clear shift in the latency distribution across operators after running the models on the GPU. GEMM operators dominated the computation for all the classification models running on CPU only platforms. Upon enabling GPU computations, the latency to run GEMMs decreased causing the NonGEMM operators to occupy a considerable proportion of the total execution time. For a batch size of 1, the proportion of time spent to compute NonGEMM operators for ViT-b16 and ViT-l16 increases from 23.5% and 18% when running on a CPU only platform to 60% and 55% respectively on the data center GPU platform. Similarly for the workstation GPU system, the NonGEMM operators execution time proportion increases to 56% and 45% for ViT-b16 and ViT-l16 to almost split the total execution time evenly with GEMM operators. For the three

Table 4. NONGEMM BENCH Model aliases used in Figure 9 and Figure 11.

Models	Batch Size	Model Alias
ViT Base 16	1	Vt-b b-1
	8	Vt-b b-8
ViT large 16	1	Vt-l b-1
	8	Vt-l b-8
Swin Transformer tiny	1	Sw-t b-1
	8	Sw-t b-8
Swin Transformer small	1	Sw-s b-1
	8	Sw-s b-8
Swin Transformer base	1	Sw-b b-1
	8	Sw-b b-8
FasterRCNN	1	FRCNN b-1
	2	FRCNN b-2
	8	FRCNN b-8
MaskRCNN	1	MRCNN b-1
	2	MRCNN b-2
	8	MRCNN b-8
DETR	2	DETR b-2
GPT2	1	gpt2 b-1
	64	gpt2 b-64
GPT2 Large	1	gpt2-L b-1
	64	gpt2-L b-64
GPT2 X-Large	1	GPT2-XL b-1
Llama2-7B	1	Llama2-7b b-1
Bert	1	bert b-1
	64	bert b-64

Swin transformers with a batch size of 1, the GEMM operators latency proportion dropped when running the inference on both the GPU systems (datacenter and workstation). Following the trend observed in the vision transformers, the NonGEMM operators contribution to the overall latency increases as well. For example, the small Swin transformer model spends 55% of the computation time executing NonGEMM operators on the data center GPU system compared to a modest 33% contribution on the CPU only system. On the workstation GPU system, the small Swin transformer also computes NonGEMM operators for 57% of the time, a 2x increase compared to the workstation CPU system. When increasing the batch size, the latency distribution across GEMM and NonGEMM operators of classification models running on GPU follows the trend observed for a batch size of 1. However, this trend is less noticeable for the largest vision transformer, ViT huge (632M parameters). For a batch size of 8, the non-GEMM operator latency is 43% and 51% for ViT-l16 and base Swin transformer respectively (Figure 5) running on the data center GPU, an 3.9x and 3x increase compared to running on a CPU only. However, the huge vision transformer only shows a 1.25x increase in the latency proportion of non-GEMM operators when accelerating the inference on the GPU.

The non-GEMM operators with the most significance to the execution time of classification models are presented in Figure 9. As shown in Table 5, Normalization operators are the most expensive non-GEMM operator in classification models when running on the data center GPU. It accounts for 19.1% of the total execution time on average. Figure 9 and Figure 11 show that Arithmetic and Memory operators are also becoming expensive on GPU systems.

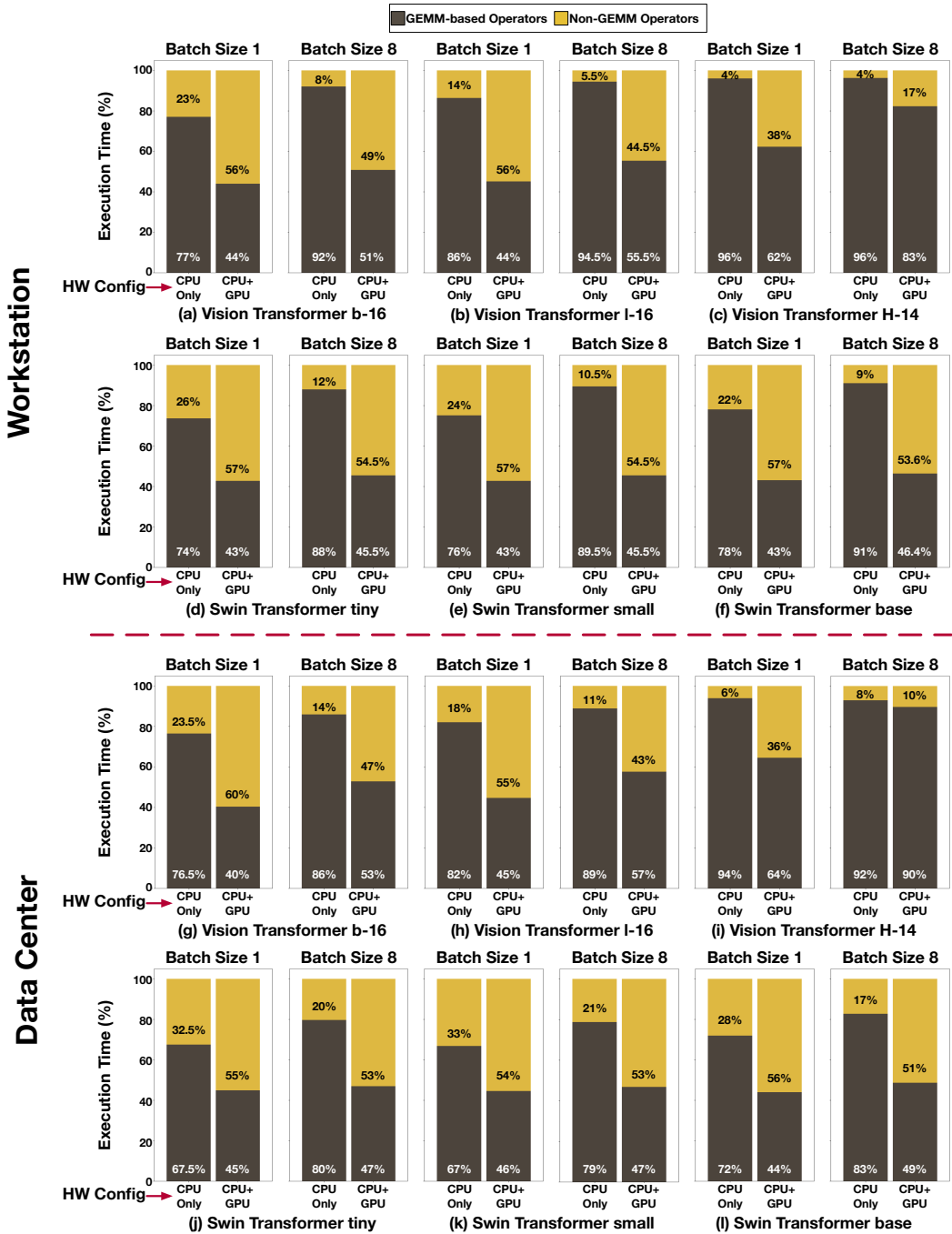


Fig. 5. The breakdown between GEMM and NonGEMM operators for image classification workloads.

Based on NonGEMM BENCH collected data, image classification models are spending more time on NonGEMM operators on GPU systems with an average of 55% for the evaluated models.

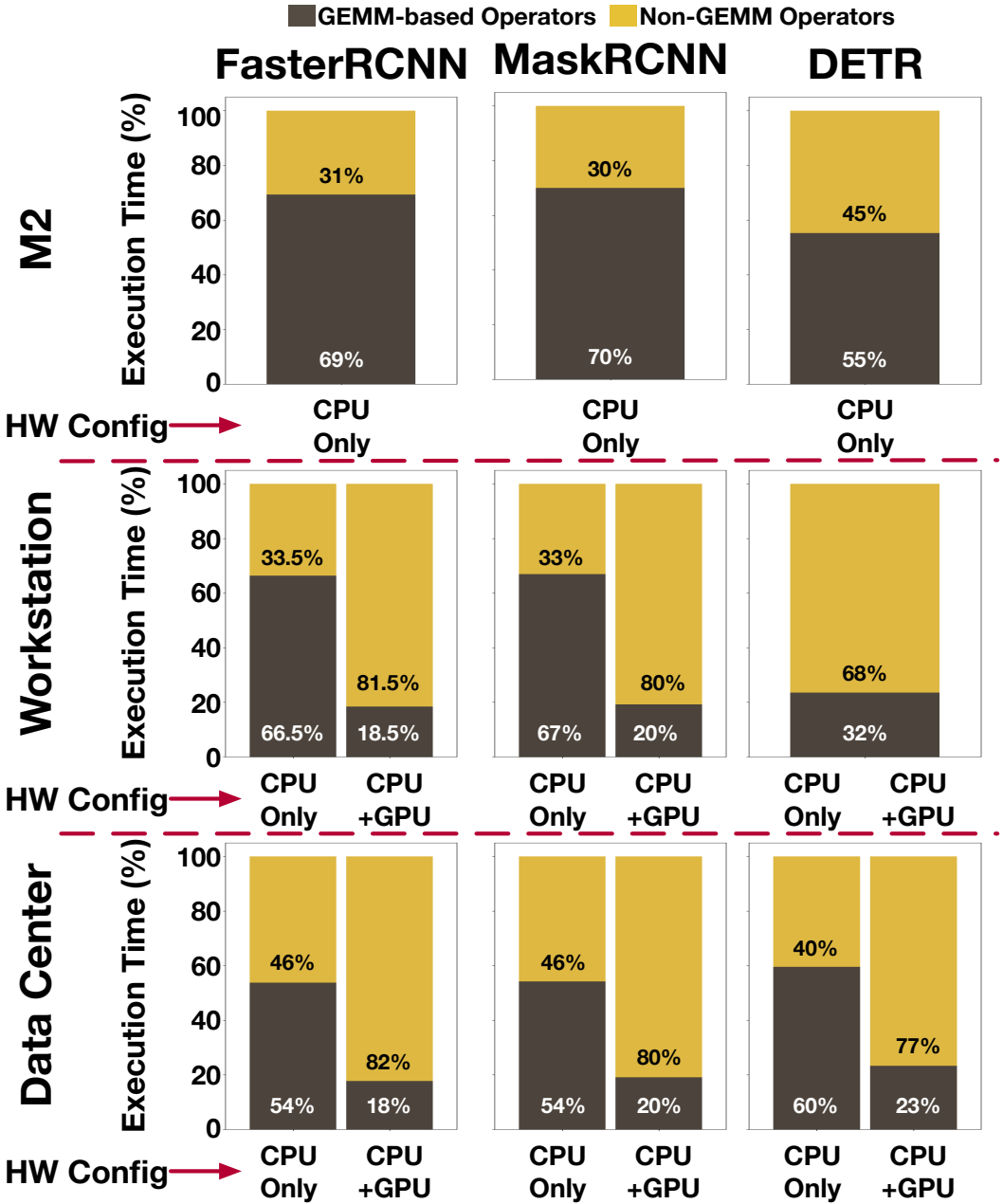


Fig. 6. The breakdown between GEMM and NonGEMM operators for object detection workloads.

4.2 Object Detection

Similar to image classification, non-GEMM operators latency becomes more noticeable when running the models on GPU systems. On the data center, NonGEMM operators dominated the execution time of FasterRCNN by consuming 82% of the total inference time when we accelerate the

workload compared to 46% when running the CPU only (Figure 6). DETR and MaskRCNN showed a similar behavior after acceleration, with a 2x increase in the time spend on non-GEMM operators. DETR computed NonGEMM operators for 77% of the inference time on the data center GPU, while MaskRCNN spent 80% on the data center and workstation GPUs. For object detection models, Normalization operators exhibit the highest execution time followed by activation and memory operators as indicated in (Figure 9). All detection models in NONGEMM BENCH use normalization functions with custom implementations that do not leverage available library normalization kernels. This leads to additional overhead caused by launching and running multiple micro-kernels to execute the normalization function. Overall, the evaluation data shows that detection models get dominated by NonGEMM operators (78%) when executing the workloads on a GPU system.

4.3 Segmentation

Interestingly, GEMM and NonGEMM operators take similar proportions of the execution time when running on the data center and workstation CPU. We notice in Figure 7 that the runtime for the Segformer model is slightly dominated by NonGEMM operators on the workstation and data center CPUs. The execution time follows a similar split between GEMM and NonGEMM operators on the mobile GPU platform as well.

4.4 Language Models

On the mobile GPU, GPT2 and Bert executed NonGEMM operators for 77% and 70% of the time with a 1.8x and 2.95x increase from the CPU system respectively when running on a single batch as indicated in Figure 8. For GPT2-large, the NonGEMM operators clearly dominated the execution time on GPU systems as well. Across the three GPU HW classes, non-GEMM operators occupy a higher ratio of execution time (76% on average). Across GPU platforms and for a batch size of 1, Figure 8 highlights the NonGEMM operators domination of the runtime. Table 5 show that Activation (23% on GPT2) and element wise arithmetic (20% on Bert) operators are the most expensive non-GEMM operators in language models running on GPU.

4.4.1 Large Language Models. Large language models latency is dominated by GEMMs when running on Data center and mobile M2 CPUs (Figure 10), consisting of 79% of the total inference time on average across platforms. When utilizing the GPU, the GEMM latency no longer bottlenecks the total execution time. The GEMM operators time drops to 30% and 22% for Llama2-7b and GPT2-XLarge respectively with non-GEMM operators executing for 74% on the GPU configuration. Figure 12 breaks down the execution time of the large language models and suggests that the bottleneck are activation, arithmetic and memory operators. Element-wise arithmetic operators are the most expensive NonGEMM operators for Llama2-7b accounting for 23% of the total runtime (Table 5, while activation functions occupy 23% of GPT2-XL total execution time.

GPT2 models implement their own GELU activation in the Hugging Face library which does not have a direct mapping to a GELU GPU kernel when running in Pytorch eager mode. This leads to additional overheads when launching different kernels running to compute the activation function. Similarly, Llama uses a normalization function that does not map to a GPU kernel in eager Pytorch which leads to similar overheads that increase the latency of the non-GEMM operators.

4.5 Key Observations

- **Accelerating the models using GPUs shifts the execution time distribution across operators accentuating the proportion of NonGEMM operators.** We average the execution time proportions for GEMM and NonGEMM operators across all the NONGEMM

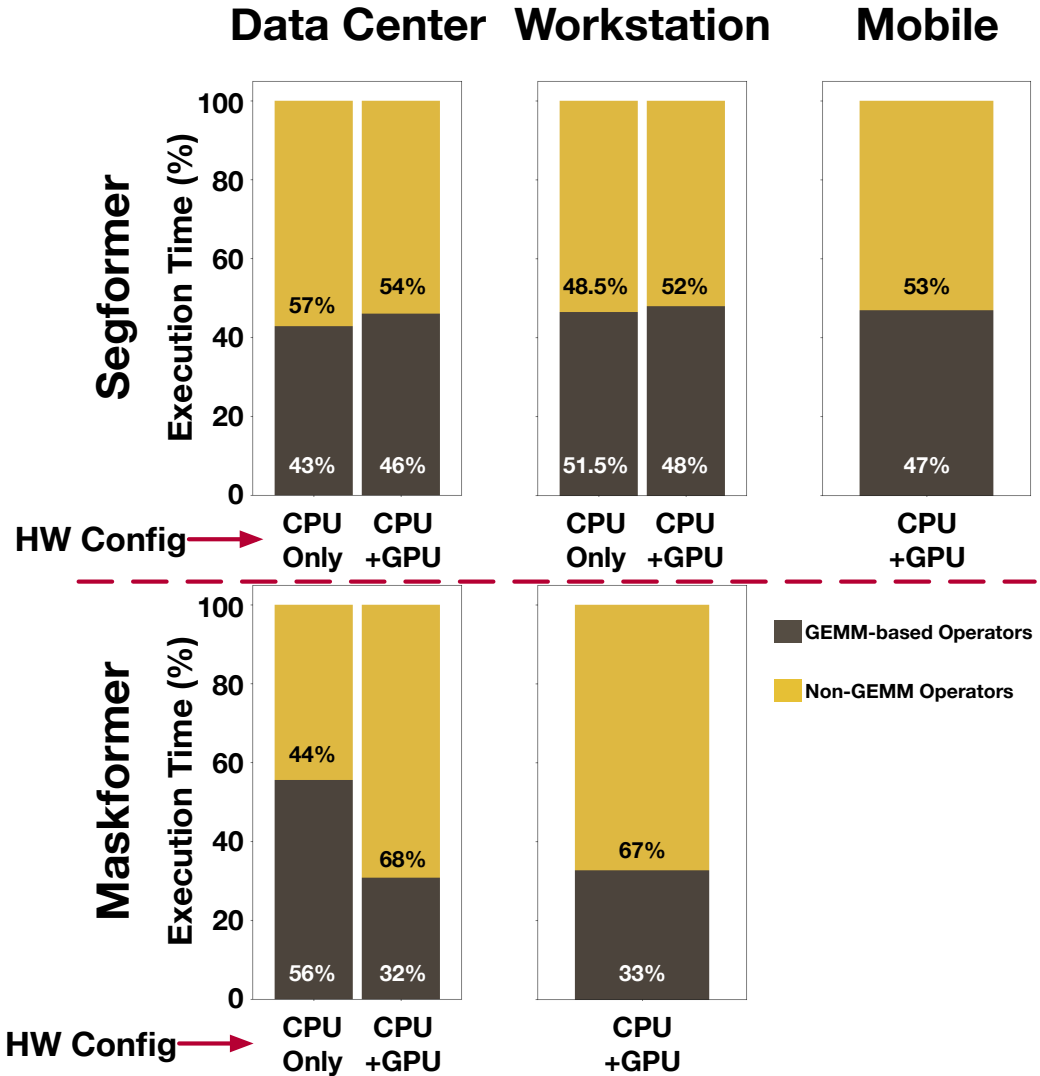


Fig. 7. The breakdown between GEMM and NonGEMM operators for segmentation workloads.

BENCH experiments (percentages shown in Figure 5, Figure 6, Figure 7, Figure 8, Figure 10). The average percentage of total inference time spent on computing the NonGEMM operators increases from 27% across CPU systems to 55% across GPU accelerated platforms.

- **NonGEMM operators' total latency portion is increasing when running the model on GPU irrespective of the grade of the GPU.** NONGEMM BENCH case studies confirmed the increase of the significance of NonGEMM operators latency on the three evaluation GPUs.
- **The significance of NonGEMM operators to the total runtime has increased when accelerating the inference on GPUs for models with various architectures and targeting different applications and task domains.**

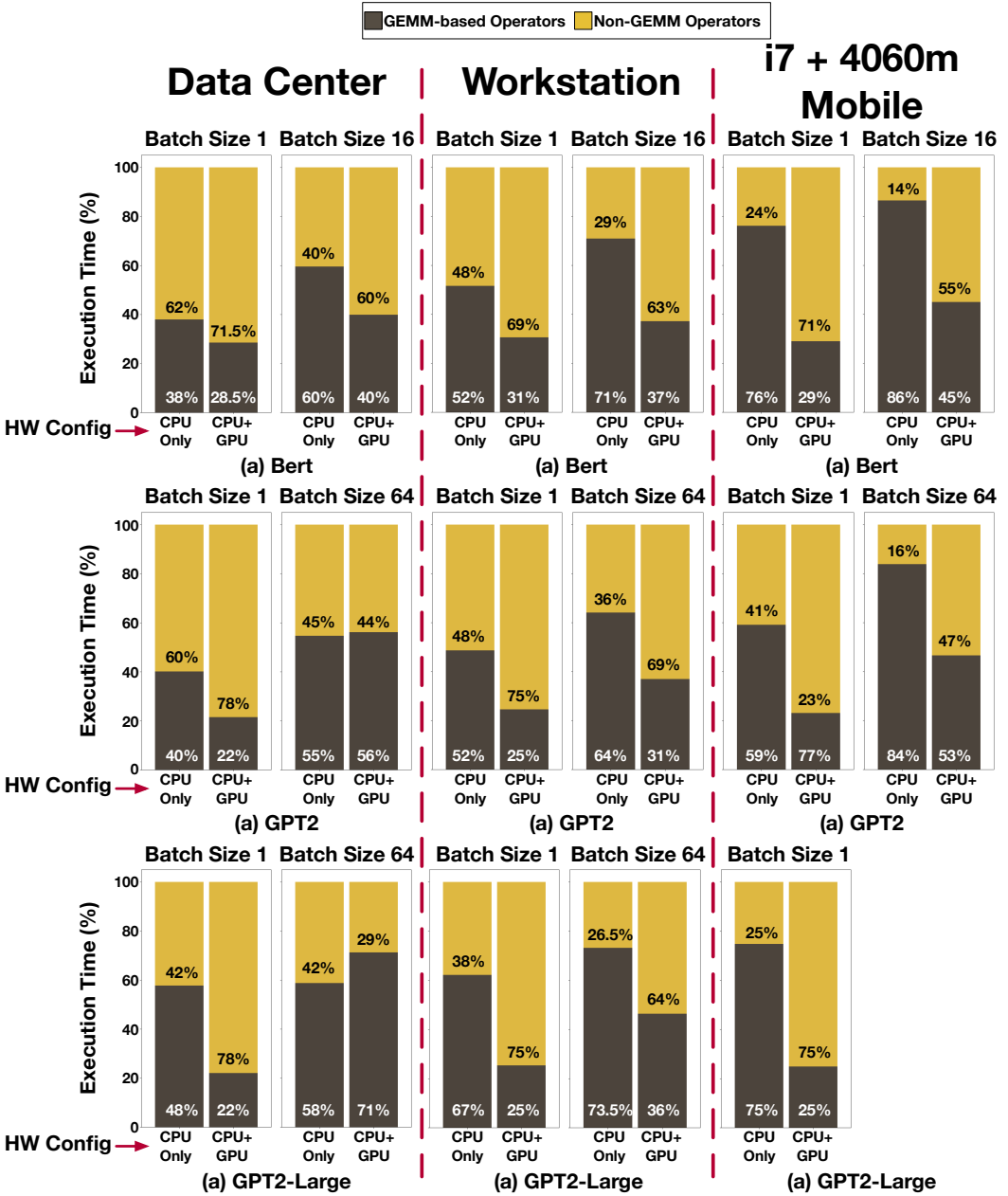


Fig. 8. The breakdown between GEMM and NonGEMM operators for language models workloads.

- **The most expensive NonGEMM operators after acceleration are not identical across models from different applications domains.** Table 5, Figure 9 and Figure 11 summarize the percentage of execution time occupied by NonGEMM operators. In IC models, Normalization operators occupy the highest proportion of execution time, with an average of 18.4%. In

Table 5. NONGEMM BENCH Most Expensive NonGEMM Operator Group for selected NONGEMM BENCH Models Running on Data Center GPU Platform.

Application	Models	Batch Size	Operator Group	% of Exec. Time
Image Classification	ViT Base 16	1	Normalization	20
		8	Normalization	17
	ViT large 16	1	Normalization	20.5
		8	Elem-Wise Arithmetic	17
	Swin Transformer tiny	1	Normalization	19
		8	Normalization	18.5
	Swin Transformer small	1	Normalization	18
		8	Normalization	17
	Swin Transformer base	1	Normalization	18
		8	Normalization	18
Object Detection	FasterRCNN	1	Normalization	60.5
		2	Normalization	59
		8	Normalization	49
	MaskRCNN	1	Normalization	58
		2	Normalization	56
		8	Normalization	49
DETR	2	Normalization	40	
Language Models	GPT2	1	Activation	23
		64	Activation	16
	GPT2 X-Large	1	Activation	23
		64	Activation	9
	Llama2-7B	1	Elem-Wise Arithmetic	23
	Bert	1	Elem-Wise Arithmetic	20
		64	Elem-Wise Arithmetic	10

language models, Activation and Element-wise Arithmetic operators are the most expensive NonGEMM operators. They respectively account for 17.75% and 17.6% of the total execution.

- **NonGEMM operators could be a potential new source of optimization to explore when designing systems for ML.** The results presented by NONGEMM BENCH align with the state of art work suggesting a novel architecture to accelerate NonGEMM operators [11].

5 RELATED WORKS

ML workloads are rapidly evolving and are becoming more integrated in various daily applications spanning different domains. Ensuring the best performance possible of these workloads is of high importance to guarantee the quality of service to the application user. Therefore, researchers have put a significant effort in creating benchmarks to evaluate the performance of workloads from different domains and understand their behavior across different platforms.

DeepBench [26] studies the performance of a very specific subset of kernels and operators. While it may provide some useful optimization insights at the operator level, it fails to capture the effect of operators when running the model end to end.

MLPerf [23] is an industry standard state of the art inference benchmark. It offers a framework to measure the end to end performance of models on platforms ranging from high performance computers to mobile devices. While it is ideal to measure end to end inference, MLPerf only support a handful of models and does not provide an operator level performance breakdown.

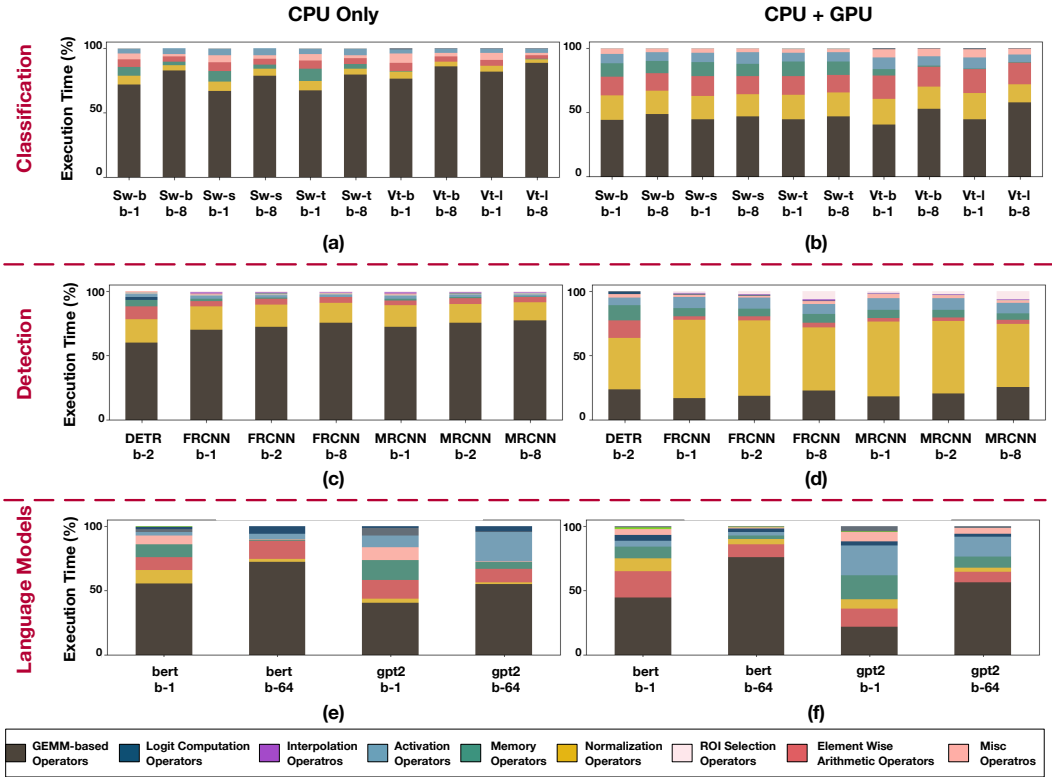


Fig. 9. Breaking down the execution time of models running on the Data Center (CPU only) and (CPU + GPU) configurations across operator groups.

TorchBench [12] presents a comprehensive benchmark suite for the Pytorch framework consisting of a large number of DL models. However, it is mainly designed to analyze the Pytorch software stack and identify optimizations specific to it.

LongTail Bench [19] is a micro benchmark that studies the operators without a specific compute library implementation. It focuses on domain specific operators from CV models. It collects the performance metrics of each operator by running it in a standalone fashion and feeding it synthetic data. Despite shedding light on non-usually studied operators, LongTail Bench isolates the operator and evaluates it on synthetically generated data, hence, failing to capture the complexities of running the operators within a model on real world data.

Given the limitations current state of the art benchamrks, and based on the results shown in Section 4, we motivate the need for NONGEMM BENCH to complete the missing features in existing benchmarking works specified in Table 6. NONGEMM BENCH is an easily extensible popularity driven benchmark that provides a performance breakdown at the operator level of popular ML models evaluating inputs from real datasets.

6 CONCLUSION

In this work, we focus on analyzing NonGemm operators in popular machine learning models. We construct NONGEMM BENCH using popular models reflecting realistic use scenarios to capture

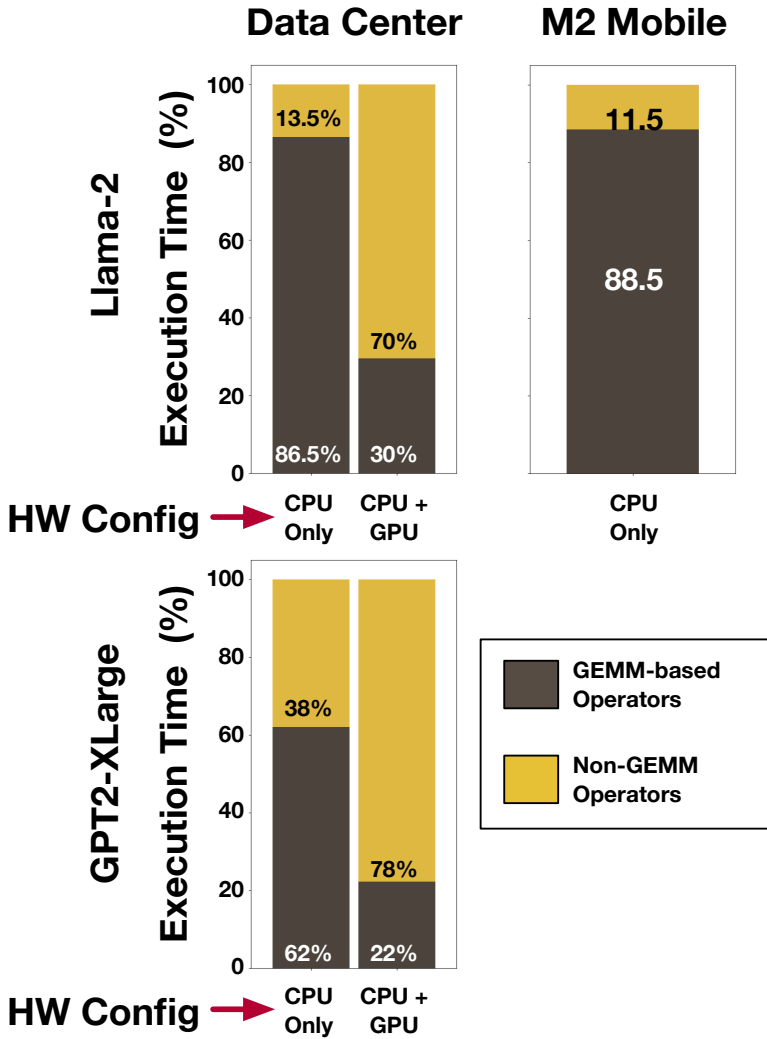


Fig. 10. The breakdown between GEMM and NonGEMM operators for large language models workloads.

Table 6. Comparing NonGEMM BENCH with existing benchmarks.

Benchmark	Latency Breakdown	Popularity Driven	Microbenchmark	Real dataset driven	Plug-model-and-profile
MLPerf [23]				✓	
LongTail [19]			✓		
TorchBench [12]		✓		✓	
NonGEMM BENCH	✓	✓	✓	✓	✓

the performance of NonGEMM operators. We evaluate NonGEMM BENCH on different hardware platforms to offer the community insights on the performance of accelerated ML workloads and potential new optimization opportunities.

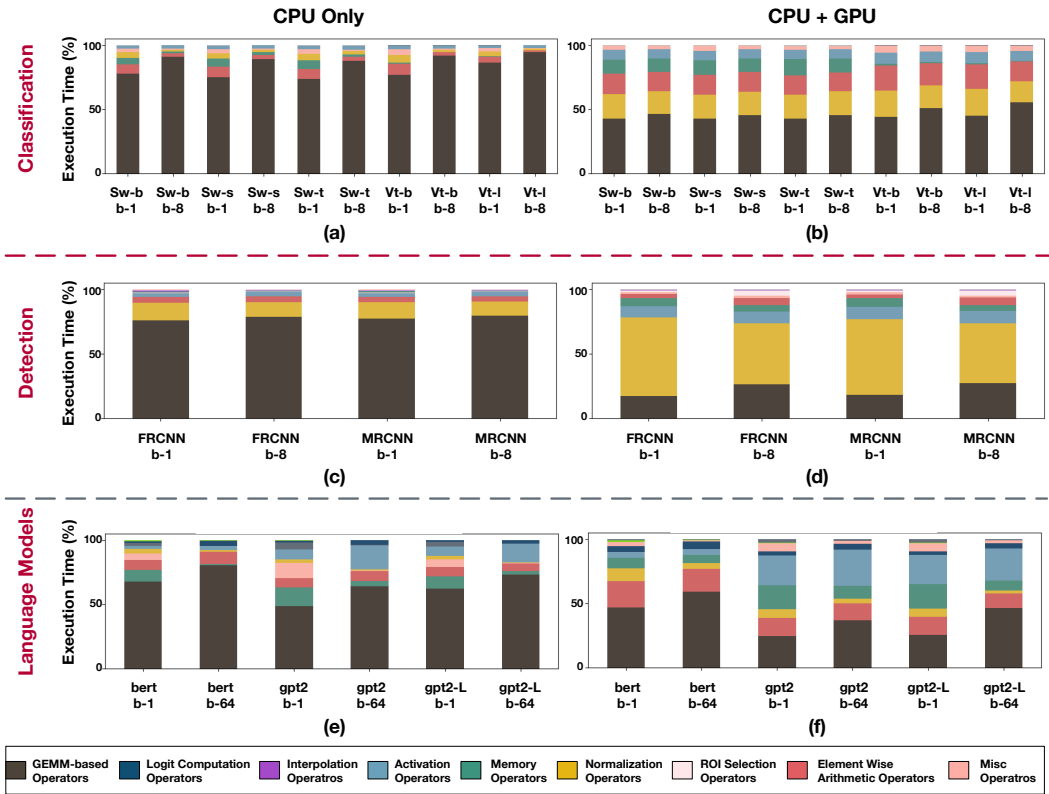


Fig. 11. Breaking down the execution time of models running on the workstation (CPU only) and (CPU + GPU) configurations across operator groups.

REFERENCES

- [1] Hugging face models hub. <https://huggingface.co/models>. Accessed on March 8, 2024.
- [2] Hugging face models hub - object detection. https://huggingface.co/models?pipeline_tag=object-detection&sort=downloads. Accessed on March 8, 2024.
- [3] Hugging face models hub - text generation. https://huggingface.co/models?pipeline_tag=text-generation&sort=downloads. Accessed on March 8, 2024.
- [4] WikiText-2 Dataset. = "<https://huggingface.co/datasets/wikitext>". Accessed on April 12, 2024.
- [5] Josh Achiam, Steven Adler, Sandhini Agarwal, Lama Ahmad, Ilge Akkaya, Florencia Leoni Aleman, Diogo Almeida, Janko Altenschmidt, Sam Altman, Shyamal Anadkat, et al. Gpt-4 technical report. *arXiv preprint arXiv:2303.08774*, 2023.
- [6] Jimmy Lei Ba, Jamie Ryan Kiros, and Geoffrey E Hinton. Layer normalization. *arXiv preprint arXiv:1607.06450*, 2016.
- [7] Nicolas Carion, Francisco Massa, Gabriel Synnaeve, Nicolas Usunier, Alexander Kirillov, and Sergey Zagoruyko. End-to-end object detection with transformers. In *European conference on computer vision*, pages 213–229. Springer, 2020.
- [8] Bowen Cheng, Alex Schwing, and Alexander Kirillov. Per-pixel classification is not all you need for semantic segmentation. *Advances in Neural Information Processing Systems*, 34:17864–17875, 2021.
- [9] Sharan Chetlur, Cliff Woolley, Philippe Vandermersch, Jonathan Cohen, John Tran, Bryan Catanzaro, and Evan Shelhamer. cudnn: Efficient primitives for deep learning. *arXiv preprint arXiv:1410.0759*, 2014.
- [10] J. Deng, W. Dong, R. Socher, L.-J. Li, K. Li, and L. Fei-Fei. ImageNet: A Large-Scale Hierarchical Image Database. In *CVPR09*, 2009.
- [11] Soroush Ghodrati, Sean Kinzer, Hanyang Xu, Rohan Mahapatra, Yoonsung Kim, Byung Hoon Ahn, Dong Kai Wang, Lavanya Karthikeyan, Amir Yazdanbakhsh, Jongse Park, Nam Sung Kim, and Hadi Esmaeilzadeh. Tandem processor:

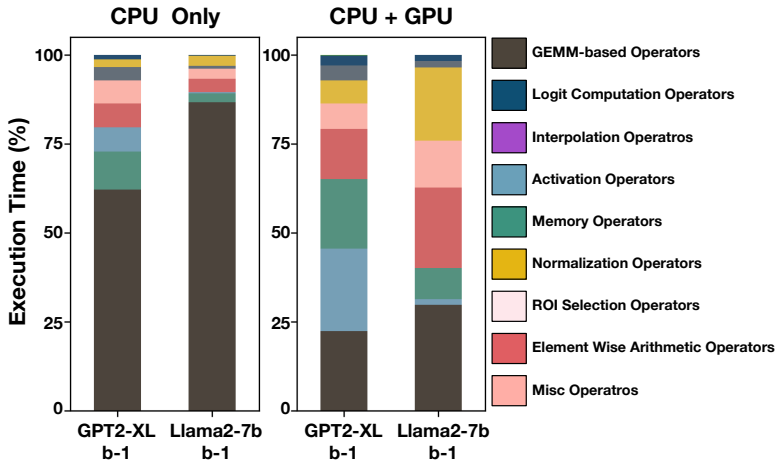


Fig. 12. The operator groups dominating the execution time of GPT2-XL and Llama-2 on running on the data center GPU system with a batch size of 1.

Grappling with emerging operators in neural networks. In *Proceedings of the 29th ACM International Conference on Architectural Support for Programming Languages and Operating Systems*, 2024.

- [12] Yueming Hao, Xu Zhao, Bin Bao, David Berard, Will Constable, Adnan Aziz, and Xu Liu. Torchbench: Benchmarking pytorch with high api surface coverage. *arXiv preprint arXiv:2304.14226*, 2023.
- [13] Kaiming He, Georgia Gkioxari, Piotr Dollár, and Ross Girshick. Mask r-cnn. In *Proceedings of the IEEE international conference on computer vision (ICCV)*, pages 2961–2969, 2017.
- [14] Kaiming He, Xiangyu Zhang, Shaoqing Ren, and Jian Sun. Deep residual learning for image recognition. In *Proceedings of the IEEE conference on computer vision and pattern recognition*, pages 770–778, 2016.
- [15] Dan Hendrycks and Kevin Gimpel. Gaussian error linear units (gelu). *arXiv preprint arXiv:1606.08415*, 2016.
- [16] Sergey Ioffe and Christian Szegedy. Batch normalization: Accelerating deep network training by reducing internal covariate shift. In *International conference on machine learning*, pages 448–456. pmlr, 2015.
- [17] Jacob Devlin Ming-Wei Chang Kenton and Lee Kristina Toutanova. Bert: Pre-training of deep bidirectional transformers for language understanding. In *Proceedings of NAACL-HLT*, pages 4171–4186, 2019.
- [18] Alexander Kolesnikov, Alexey Dosovitskiy, Dirk Weissenborn, Georg Heigold, Jakob Uszkoreit, Lucas Beyer, Matthias Minderer, Mostafa Dehghani, Neil Houlsby, Sylvain Gelly, Thomas Unterthiner, and Xiaohua Zhai. An image is worth 16x16 words: Transformers for image recognition at scale. In *Proceedings of the International Conference on Learning Representations (ICLR)*, 2021.
- [19] Xiuhong Li, Shengen Yan, Lijuan Jiang, Ping Xu, Jinming Ma, Xingcheng Zhang, and Dahua Lin. Longtail-bench: A benchmark suite for domain-specific operators in deep learning. In *2022 IEEE International Symposium on Workload Characterization (IISWC)*, pages 282–295. IEEE, 2022.
- [20] Tsung-Yi Lin, Michael Maire, Serge Belongie, James Hays, Pietro Perona, Deva Ramanan, Piotr Dollár, and C Lawrence Zitnick. Microsoft coco: Common objects in context. In *Computer Vision—ECCV 2014: 13th European Conference, Zurich, Switzerland, September 6–12, 2014, Proceedings, Part V 13*, pages 740–755. Springer, 2014.
- [21] Ze Liu, Yutong Lin, Yue Cao, Han Hu, Yixuan Wei, Zheng Zhang, Stephen Lin, and Baining Guo. Swin transformer: Hierarchical vision transformer using shifted windows. In *Proceedings of the IEEE/CVF international conference on computer vision (ICCV)*, pages 10012–10022, 2021.
- [22] Alec Radford, Jeffrey Wu, Rewon Child, David Luan, Dario Amodei, Ilya Sutskever, et al. Language models are unsupervised multitask learners. *OpenAI blog*, 1(8):9, 2019.
- [23] Vijay Janapa Reddi, Christine Cheng, David Kanter, Peter Mattson, Guenther Schmuelling, Carole-Jean Wu, Brian Anderson, Maximilien Breughe, Mark Charlebois, William Chou, et al. Mlperf inference benchmark. In *2020 ACM/IEEE 47th Annual International Symposium on Computer Architecture (ISCA)*, pages 446–459. IEEE, 2020.
- [24] James Reed, Zachary DeVito, Horace He, Ansley Ussery, and Jason Ansel. Torch. fx: Practical program capture and transformation for deep learning in python. *Proceedings of Machine Learning and Systems*, 4:638–651, 2022.

- [25] Shaoqing Ren, Kaiming He, Ross Girshick, and Jian Sun. Faster r-cnn: Towards real-time object detection with region proposal networks. *Advances in neural information processing systems*, 28, 2015.
- [26] Baidu Research. Deepbench, 2016.
- [27] Mark Sandler, Andrew Howard, Menglong Zhu, Andrey Zhmoginov, and Liang-Chieh Chen. Mobilenetv2: Inverted residuals and linear bottlenecks. In *Proceedings of the IEEE conference on computer vision and pattern recognition (CVPR)*, pages 4510–4520, 2018.
- [28] Hugo Touvron, Louis Martin, Kevin Stone, Peter Albert, Amjad Almahairi, Yasmine Babaei, Nikolay Bashlykov, Soumya Batra, Prajjwal Bhargava, Shruti Bhosale, et al. Llama 2: Open foundation and fine-tuned chat models. *arXiv preprint arXiv:2307.09288*, 2023.
- [29] Ashish Vaswani, Noam Shazeer, Niki Parmar, Jakob Uszkoreit, Llion Jones, Aidan N Gomez, Łukasz Kaiser, and Illia Polosukhin. Attention is all you need. *Advances in neural information processing systems*, 30, 2017.
- [30] Enze Xie, Wenhai Wang, Zhiding Yu, Anima Anandkumar, Jose M Alvarez, and Ping Luo. Segformer: Simple and efficient design for semantic segmentation with transformers. *Advances in Neural Information Processing Systems*, 34:12077–12090, 2021.
- [31] Biao Zhang and Rico Sennrich. Root mean square layer normalization. *Advances in Neural Information Processing Systems*, 32, 2019.